Characteristics and trends of land subsidence in Tanggu, Tianjin, China

R.L. Hu · S.J. Wang · C.F. Lee · M.L. Li

Abstract Land subsidence in the Tanggu area is directly related to withdrawal of shallow groundwater within a depth of 300 m. The main strata responsible for the subsidence are at a depth of between 136 and 300 m. The contribution to subsidence made by the clayey soils is dierent from that of the sandy soils, as the former is related to the seasonal dropping of the water table while the latter is associated with annual changes. In addition, while there is a clear correlation between the accumulative groundwater extraction and the accumulative subsidence, this linear relationship is not obvious between annual extraction and annual subsidence. A case study in Tanggu, Tianjin, is presented in order to demonstrate a proposed computational model to predict land subsidence – the Optimization Model for Land Subsidence (OMLS).

Résumé La subsidence aectant la région de Tanggu résulte directement de l'exploitation d'eaux souterraines jusqu'à 300 m de profondeur. Les formations géologiques en cause se situent entre 136 et 300 m de profondeur. La contribution des formations argileuses au phénomène de subsidence est différente de celle des sols sableux, les premières répondant aux abaissements saisonniers de la surface piézométrique, les dernières jouant un rôle en rapport avec les fluctuations pluri-annuelles. De plus, alors qu'il y a une relation linéaire claire, sur une longue période, entre le volume total d'eau pompée et le tassement total mesuré, cette corrélation n'est pas évidente lorsque l'on compare le pompage annuel et le tassement annuel. Une étude de cas à Tanggu, Tianjin est présentée, utilisant le modèle de prévision de subsidence OMLS (Optimization Model for Land Subsidence).

Keywords Land subsidence · Characteristics · Prediction · Optimization model

Mots clés Subsidence · Caractéristiques · Prévision · Modèle

Received: 17 November 2000 / Accepted: 16 May 2001
Published online: 8 September 2001

R.L. Hu (✉) · S.J. Wang
Engineering Geomechanics Laboratory,
Institute of Geology, Chinese Academy of Sciences,
Beijing, China

C.F. Lee
Department of Civil Engineering,
University of Hong Kong, Hong Kong

M.L. Li
Tianjin Bureau of Geology and Mineral Resources,
Tianjin, China

Correspondence address: R.L. Hu
Engineering Geology Section,
Institute of Geology, Chinese Acadamy of Sciences,
P.O. Box 634, Beijing 100029, China
e-mail: huruilin@mail.com
Tel.: +86-10-62008066, Fax: +86-10-62040574

Introduction

Tanggu, a coastal area in the east of Tianjin City (Fig. 1), is only some 2.0–2.4 m above sea level. With the rapidly increasing water demands for urban development and human consumption, extraction from within the city has resulted in the downtown area of Tianjin subsiding. Since 1959 the maximum accumulated subsidence has reached almost 3 m and some parts of the city are now at or slightly lower than sea level. One of the fastest subsiding areas in Tianjin City is Tanggu, which is now facing possible inundation at high storm tides. As a consequence, subsidence control is an urgent problem to which considerable attention has been paid by the Tianjin Municipality and related departments. Since the 1980s many researchers, including scientists from Belgium and Britain, have been invited to study the extent of the subsidence in downtown Tianjin City and Hangu with the result that the subsidence has been reduced to less than 10 mm/year (Tianjin Center of Geological Survey 1991; Zhang 1991). However, the subsidence in the coastal area of Tanggu is increasing due to the lack of a systematic study and effective control measures.

This paper reports on a study of the land subsidence in the coastal area of Tanggu and the attempt to develop a simple

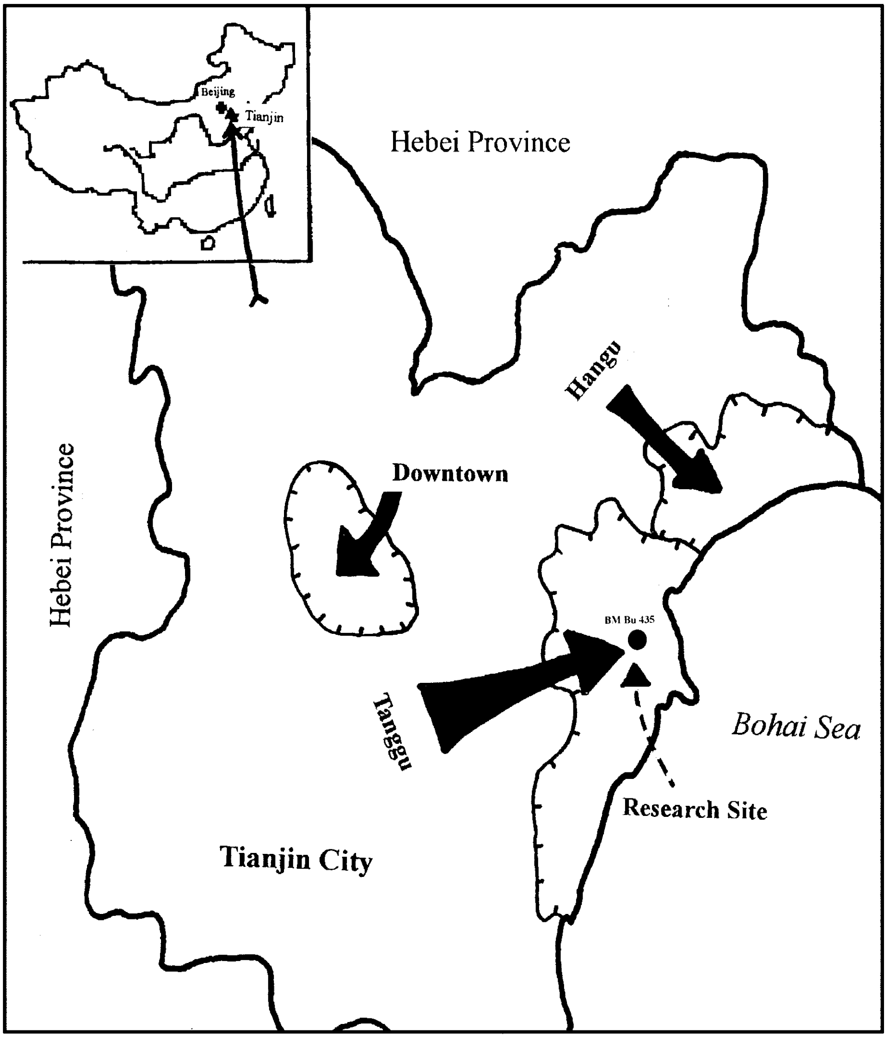

Fig. 1
Geographical location of the research area

and effective computational method to elucidate the causes and find possible mitigation measures.

Hydrogeological and engineering geological conditions

Geographical and geological settings

Tanggu is located in the northeastern coastal area of the North China Plain. The area has a continental monsoon climate, with an average annual precipitation of 600–650 mm, much less than the average annual evaporation of 1,800–1,900 mm. Both the precipitation and evaporation vary seasonally and geographically: the rain falling mainly in the northeast of the city in July, August and September while the evaporation is greatest in the southwest of the city in April and May.

Tianjin is at the junction of the Tianshan–Yinshan (latitudinal) and Neocathaysian tectonic systems. The Huanghua depression is a key structure which has developed where the Haihe and the Cangdong fault systems intersect. Although there has been no major movement in the Neocathaysian subsidence zone since the Cenozoic, because of the different rates and duration of the subsidence that occurred, the sediments vary in thickness; the Paleozoic, Mesozoic and Tertiary strata ranging between 1,000 and 8,000 m. There is no exposed bedrock in Tanggu, but the Quaternary deposits, which rest unconformably on the Tertiary strata, extend to a depth of 500–550 m.

Hydrogeology

The Haihe River flows through the area into the sea and has deposited a thick mass of loose Quaternary sediments which have complex textural structures and varying hydrogeological conditions. Aquifers are present within the interbedded Quaternary strata. Towards the south, the grain size reduces and the thickness of the deposits decreases. Here the mainly fine silts and sands are characterized by moderate permeability, slow runoff and poor recharge.

Division of aquifers and dynamic features of the water table

The aquifer system is usually divided into seven units (Table 1) related to the lithological and hydrogeological conditions. The second and third confined aquifers are the main sources of groundwater extraction in this area. Before 1984 the water table related to the third confined

Table 1
Details of the main aquifers in the research area, Tanggu, Tianjin City

Unit	Aquifer	Dominant lithology	Depth of bottom (m)	Thickness (m)	Water table				Degree of mineralization (g/l)
					Depth of water head (m)	Period for high water table	Period for low water table	Annual change (m)	
A	Phreatic aquifer	Yellow–grey porous clay and lens-shaped silts	4–6	4–6	Shallow	Varies with the seasons			1–2
B	Slightly confined aquifer	Lens-shaped silt and fine sands	15–20	9–16	1.5–5.0				2–6
C	First confined aquifer	Silt and fine sands	60–75	40–60	6–15	June–Sept	Nov–Mar	1–5	10–15
D	Second confined aquifer	Silt and fine sands	170–190	25–60	15–20		June–Aug	4–8	Upper: saline; bottom: fresh
E	Third confined aquifer	Silt and fine sands	270–310	30–55	45–65		June–Aug.	1–4	0.5
F	Fourth confined aquifer	Fine sands, silt	370–400	30–50					0.4–0.6
G	Fifth confined aquifer	Fine sands, silt	About 550	20–30	70–80				0.34–0.43

aquifer was dropping at a rate of 0.8 m/year (Fig. 2); between 1984 and1988 it remained stable, but since 1988 it has risen at a rate of 1.0 m/year. Since 1985, the water table of the second confined aquifer has gradually risen by about 5 m.

Groundwater extraction

Although the groundwater in the area was exploited before 1949, with the increase in agricultural development in the 1960s, large-scale extraction began. The annual extraction from the various confined aquifers between 1984 and 1993 is shown in Fig. 3. It can be seen that by 1993 the extraction rate had dropped to some 20% of that in 1984, largely as a result of introducing the Luanhe River water into the Tianjin area.

The groundwater is continuously exploited from certain levels and locations (mostly in the urban and industrial areas). The main exploitation is from the second and third confined aquifers which provide some 70% of the total water extracted: 46% from the second aquifer and 24% from the third. Generally, the groundwater is pumped from a depth of 100–300 m. This water is obtained for industrial, agricultural and domestic use, while the waters from below 300 m are used for geothermal development.

Land subsidence

Historical levelling data show that the annual subsidence of this area before 1959 averaged only 0.7–7.9 mm. The bench mark (BM) at the Xinghe Shipyard indicated a subsidence of 41 mm between 1941 and 1959, averaging 2.3 mm/year. However, in the 35 years since 1959 the accumulated subsidence was over 2.9 m. A notable centre of subsidence is at the juncture of Yongjiu Street, Shanghai Road and Hebei Street where the elevation dropped to 0.57 m below sea level, while a 4–5 km^2 area in the west of Tanggu has subsided almost to sea level. By the end of

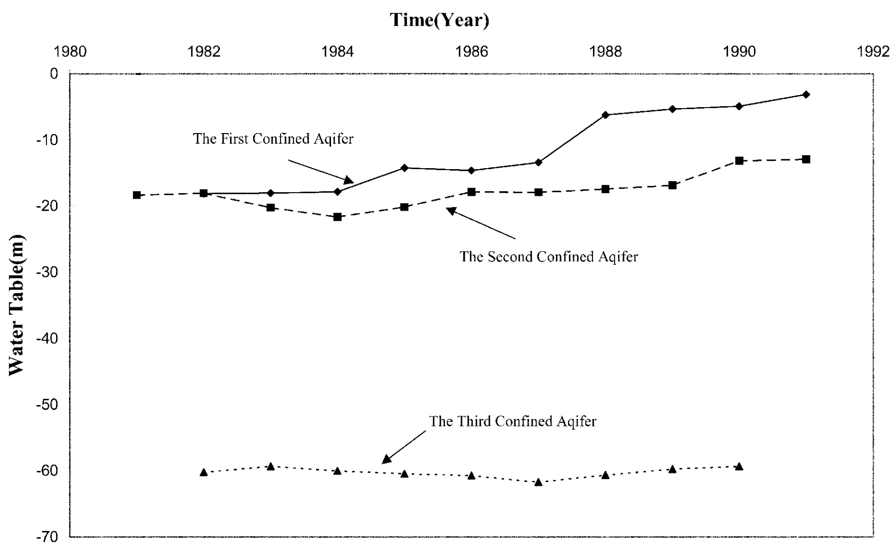

Fig. 2
Groundwater table in the first, second and third confined aquifers at Tanggu

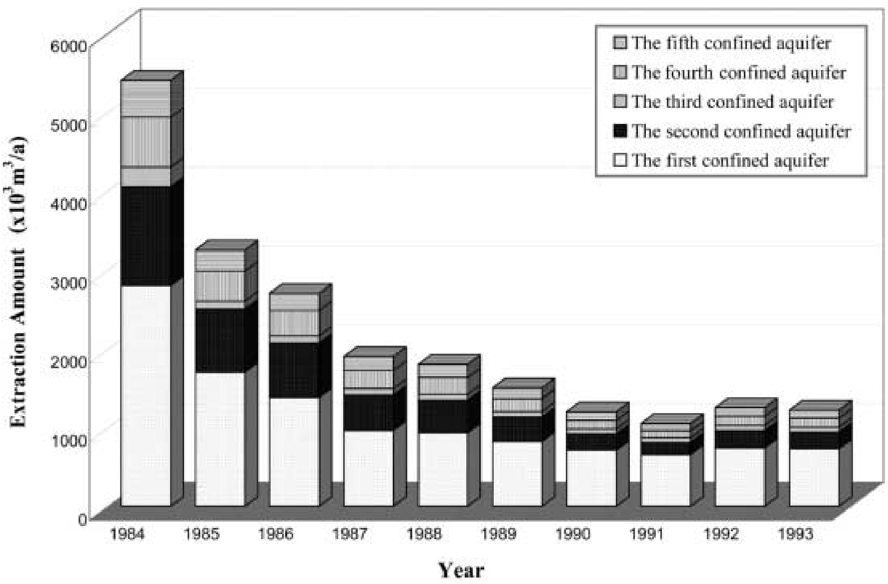

Fig. 3
Annual extraction from the major aquifers in Tanggu

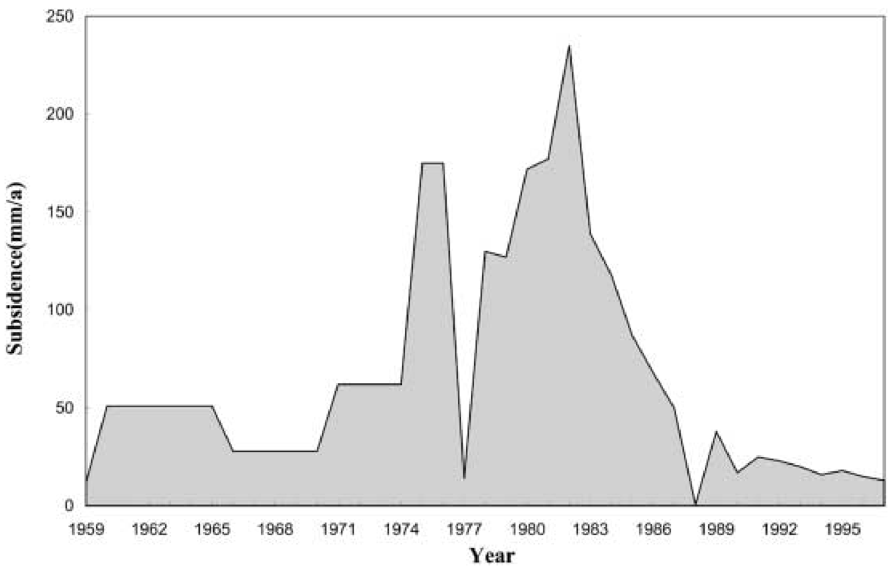

Fig. 4
Subsidence rates for bench mark Bu 435 during 1959–1997

1988 an area of more than 8 km^2 had experienced subsidence of more than 2 m and there was more than 1.5 m of subsidence over a 15 km^2 area.

Figure 4 indicates that the subsidence recorded at the bench mark for the period 1959–1997 can be divided into three main stages.

Slow subsidence (1959–1977)
Between 1959 and 1977 the subsidence varied significantly. In the early 1960s it averaged some 50 mm/year. Between 1974 and 1977 there was a period of major settlement when some 170 mm/year was experienced, but this is considered to be largely related to the influence of the Tangshan earthquake rather than groundwater exploitation.

Accelerating subsidence (1978–1982)
The subsidence rate in this period was over 100 mm/year, reaching a maximum rate of 250 mm in the early 1980s.

Attenuating subsidence (1983–1997)
As a consequence of subsidence control measures, after 1982 there was a significant decrease in the rate of extraction, and subsidence slowed such that in the 1990s it averaged only 20–30 mm/year.

Analysis of some features related to subsidence

Variation of stratum deformation with depth

Seven wire-flex extensometers have been installed in Tanggu with fixed points some 300 m below ground level. Figure 5 indicates the percentages of stratum deformations at individual points relative to the total deformation (subsidence). It can easily be seen that subsidence in the Tanggu area is largely due to deformation of layers 5, 6 and 7, at between 136 and 300 m below ground level. In total, these three layers account for some 65% of the total subsidence: layer 5 having 10–20%, layer 6 circa 20% and layer 7 some 25–30%.

From the measurements obtained at the seven wire-flex extensometers in Tianjin Alkali Mill (Fig. 6), the relative deformations associated with the three upper aquifers can be assessed, although it will be noted that there is considerable variation from one year to the next. From this it is possible to determine the percentage of deformation related to extraction from the deeper aquifers. It is clear that extraction from the third confined aquifer has the maximum influence in the upper layers, resulting in some 30% of the total subsidence compared with circa 15% associated with the second confined aquifer and less than 10% with the first. The amount of settlement related to the first confined aquifer varies significantly, dropping between 1983 and 1985, 1986 and 1988 and progressively from 1991–1997. Although the intensity of extraction from the second aquifer is slightly higher than that from the third, the subsidence contribution of the former is lower than that of the latter. Figure 6 indicates that in 1985 the second confined aquifer created the main problem and hence mitigation measures were instigated in 1985 to reduce the influence of extraction from this level. In recent years the extraction intensity has still been the largest of these three aquifers, but less than its previous value.

At present, the depth to which the stratum deformation is monitored in Tanggu is only 300 m. It can be seen from Fig. 7 that the deformation trend associated with the shallow aquifers (dashed line) is similar to the general trend of subsidence. The figure also emphasizes that most of the subsidence recorded at the surface is related to settlement at depths of less than 300 m. Measures to control land subsidence should therefore mainly be undertaken above a depth of 300 m.

Figure 8 shows that extraction from the shallow aquifers remains relatively constant at between 60 and 80% of the total extraction, while the deformation of the shallow aquifers (i.e. ground subsidence) is generally less than

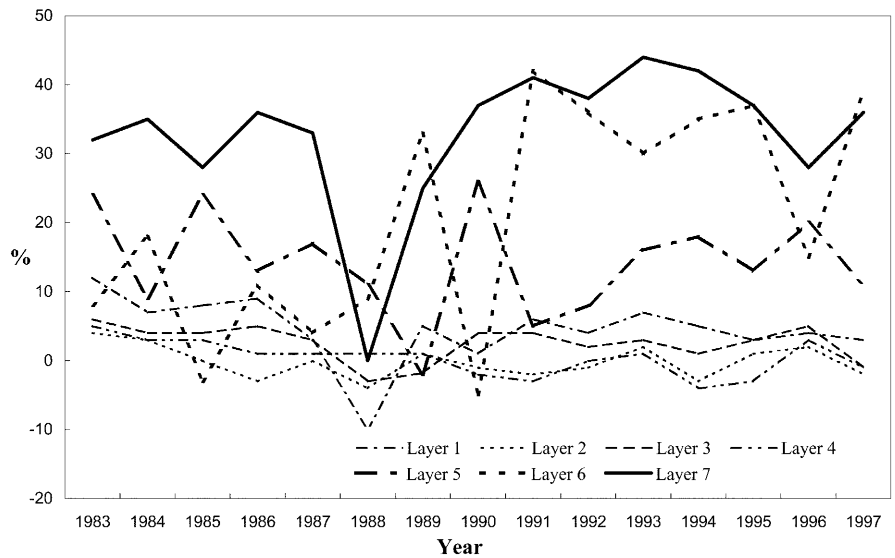

Fig. 5
Percentage of stratum deformation at the seven wire-flex extensometers relative to total subsidence

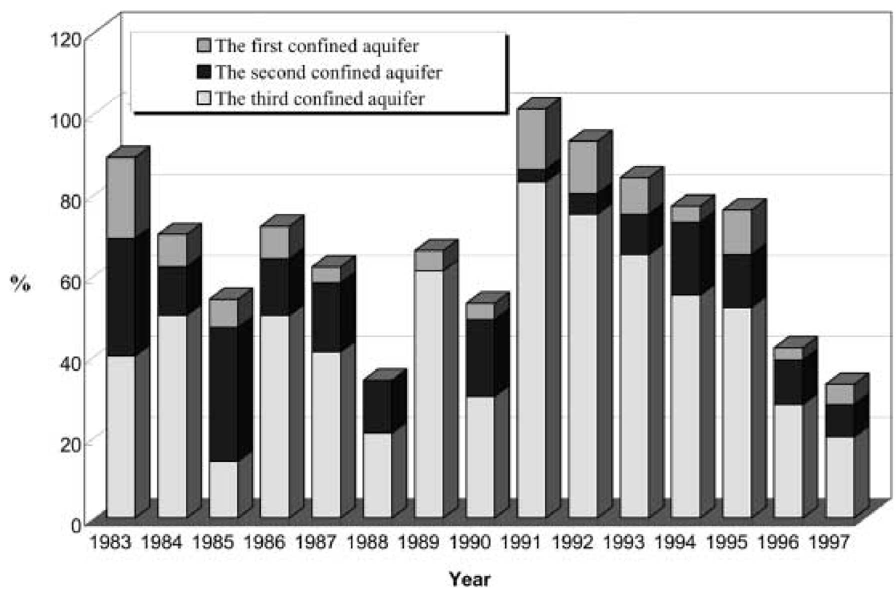

Fig. 6
Percentage of deformation of shallow aquifers at Tianjin Alkali Mill relative to total subsidence

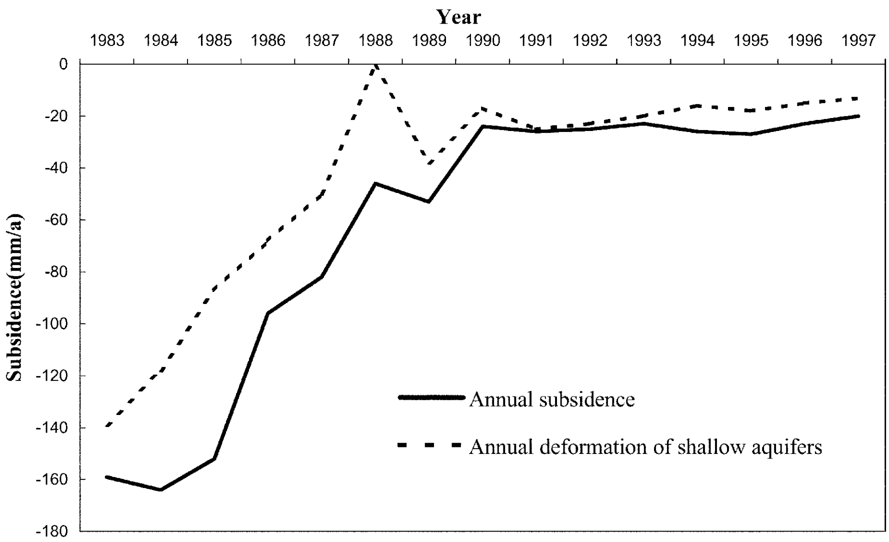

Fig. 7
Total annual subsidence and annual deformation of shallow aquifers at Tianjin Alkali Mill

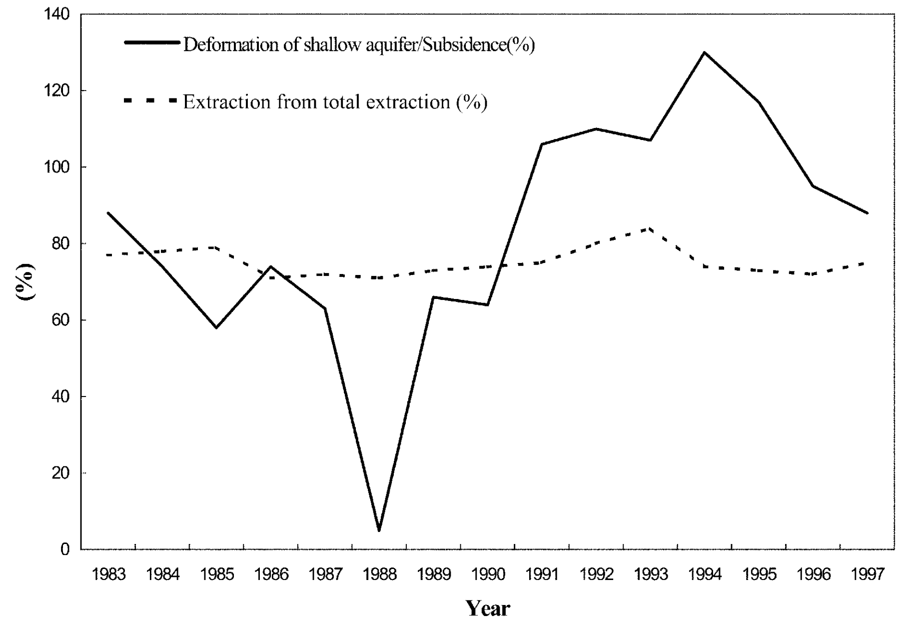

Fig. 8
Shallow deformation as a percentage of total subsidence and shallow groundwater extraction as a percentage of total extraction at Tianjin Alkali Mill

100%, i.e. there is some component from the deep aquifers although not until the early/mid 1990s.

Relationship between the water tables of the aquifers and their deformation

The lowering of the water table is the main factor leading to land subsidence. Each year, the groundwater table drops in summer during the period of peak water demand and rises in winter when the use of water is relatively less. However, there is some variation both from year to year and between the different aquifers.
This study has considered particularly the upper aquifer, the data from which are presented in Fig. 9. The diagram shows the level of the water table and the accumulated deformations that have been recorded for sandy soils and clayey soils. Sandy materials are usually considered as very sensitive to changes in groundwater conditions, with the deformation and restoration taking effect quickly when the soils are dried and subsequently saturated. As seen in Fig. 9, the accumulated deformation curve is generally similar to that of the groundwater level, although there is often a slight lapse between the ground response and the change in groundwater table. Clayey soils deform in a plastic and non-restorable manner. In view of this, the annual change in groundwater level has little effect on soil consolidation and it is only when the annual rise in the water table is considerably greater than its seasonal drop (as in 1988–1990) that there can be sufficient rehydration to result in a drop in the rate of settlement or even the ground beginning to rise (see Fig. 9).

Relationship between groundwater extraction amount and land subsidence

Figures 10 and 11 give the relationship between the annual (Fig. 10) and accumulative (Fig. 11) groundwater extrac-

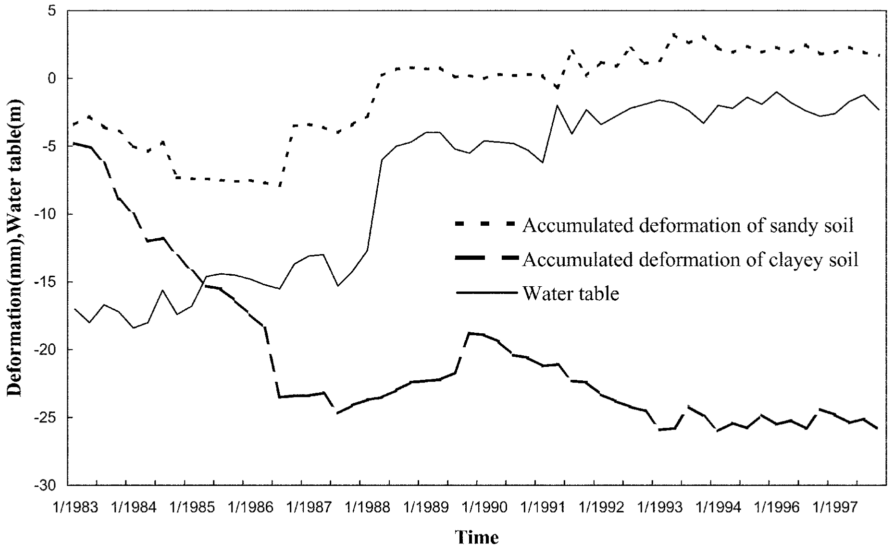

Fig. 9
Variation of groundwater table and accumulative deformation for the first confined aquifer at Tianjin Alkali Mill

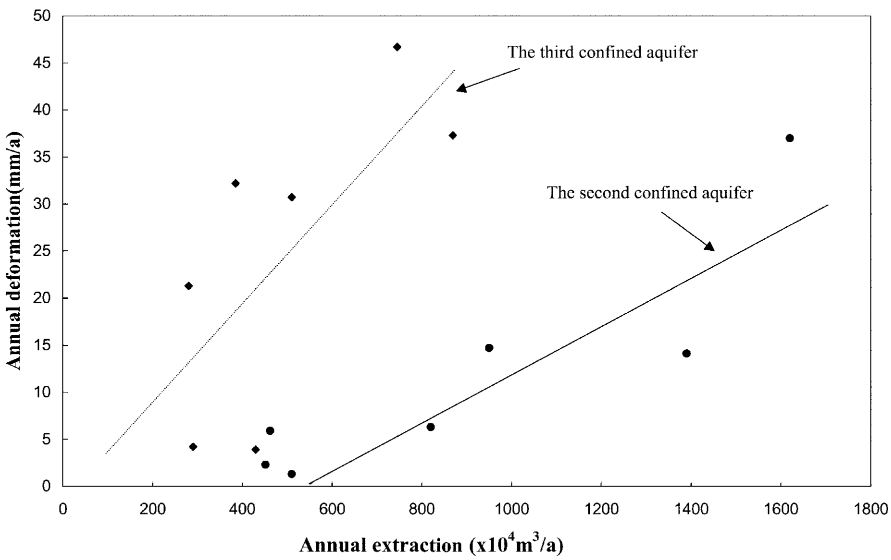

Fig. 10
Relationship between annual groundwater extraction and annual deformation of the second and third confined aquifers

tion and the deformation associated with the second and third confined aquifers. There are two possible explanations for the data in Fig. 10:

(1) there is a linear relationship between the annual extraction and annual deformation. However, for the second confined aquifer, the coefficient is only 0.89 and for the third aquifer it is 0.7; and

(2) the relationship between the annual extraction and annual deformation is non-linear. In the case of the second confined aquifer, the deformation is negligible when the extraction is less than 0.3 million m^3/year. As extraction continues to some 1.25 million m^3/year, the deformation rises gradually to some 20 mm/year, but when the extraction is increased to 1.7 million m^3/year, the rate of deformation rises rapidly to some 40 mm/year.

In the case of the third aquifer, again it is unlikely that any settlement will occur until 0.3 million m^3/year of water has been extracted, after which a very small additional amount will cause a sudden steep rise such that 0.5 million m^3/year may cause in excess of 30 mm of deformation. Above this extraction rate, the effect on settlement reduces with only approximately 45 mm/year subsidence when 1 million m^3 of groundwater is extracted.

Figure 11 shows that when the accumulated extraction is related to the accumulated deformation, a more linear trend is observed, which can be expressed by the following formulae:

For the second aquifer

$$\Sigma S_{II} = 88.89 + 0.0085 \Sigma Q_{II} (R^2 = 0.9685; S = 3.9934) \quad (1)$$

For the third aquifer

$$\Sigma S_{III} = 144.88 + 0.0511 \Sigma Q_{III} (R^2 = 0.9911; S = 7.068) \quad (2)$$

where ΣS_{II} and ΣS_{III} are the accumulative deformations of the second and third confined aquifers respectively, ΣQ_{II} and ΣQ_{III} are the accumulative groundwater extraction from the second and third confined aquifers respectively, R^2 is the regression coefficient and S is variance. The

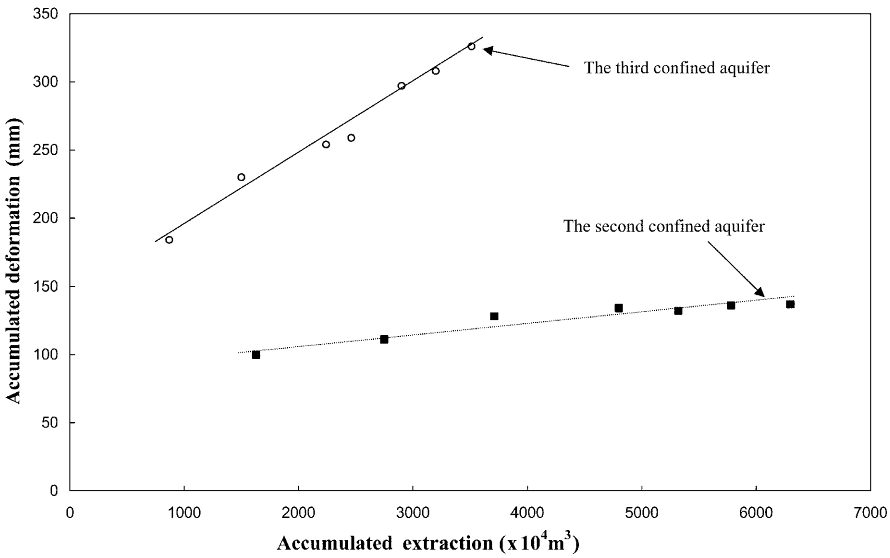

Fig. 11
Relationship between accumulative groundwater extraction and accumulative deformations of the second and third confined aquifers

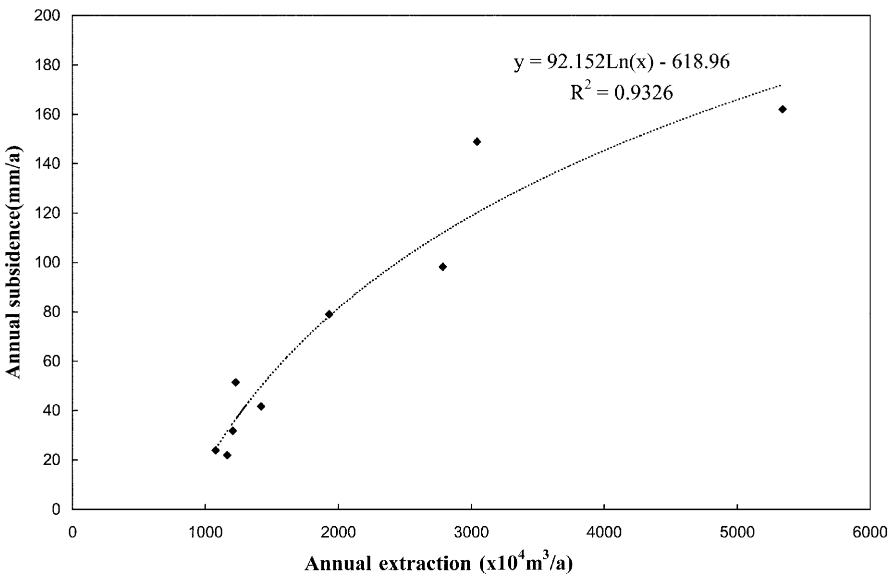

Fig. 12
Relationship between annual groundwater extraction and annual subsidence

results indicate that the effect of these accumulated values could eliminate the hysteresis deformation to a considerable extent (Xu et al. 1991).

In Tanggu the strata consist mainly of sandy and clayey soils. The hysteresis of a clayey soil has an influence on stratum deformation, but compared with the accumulative instantaneous deformation this is not significant and there is a semi-logarithmic linear relationship between the annual groundwater extraction and annual subsidence, as seen in Fig. 12. This can be expressed as:

$$S = -618.96 + 92.152\ln(Q)(R^2 = 0.9326; S = 2.6634) \quad (3)$$

where S is annual land subsidence (in mm/year) and Q is annual volume of groundwater extracted (in 10^4 m^3/year). As shown in Fig. 13, the relationship between accumulative extraction from the confined aquifers and associated accumulative ground subsidence is similar to that between the total groundwater extraction and total accumulative settlement. This may be expressed as:

$$\Sigma S = 0.0344\Sigma Q + 2087.8(R^2 = 0.977; S = 1.4334) \quad (4)$$

where ΣS is accumulative subsidence (in mm) and ΣQ is accumulative groundwater extraction in (10^4 m^3).

It is considered that the above Eq. (4) could provide a simple and reliable method of estimating land subsidence and assist in the management of groundwater resources in areas of potential subsidence.

Calculation of stratum deformation

For the calculation of stratum deformation/subsidence, models are commonly used to determine the settlement of individual layers with time to produce time-dependent

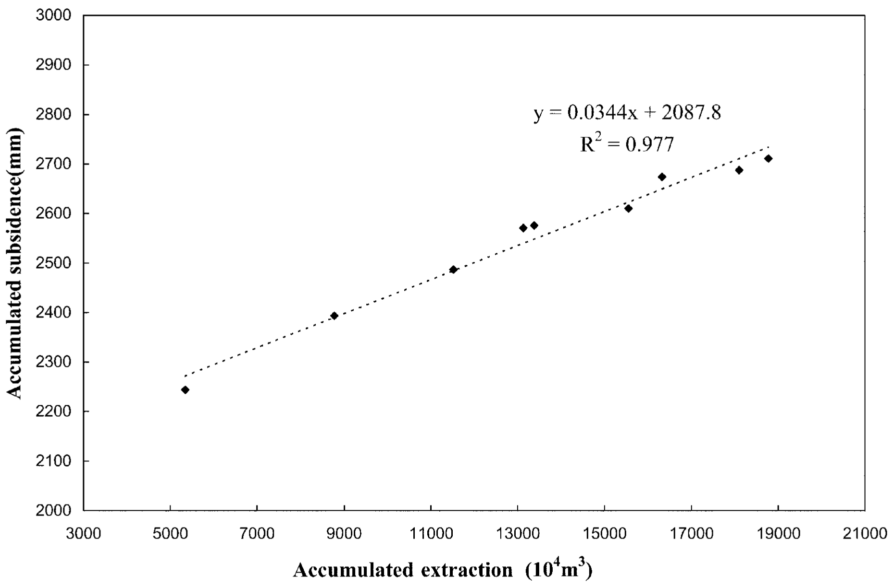

Fig. 13
Relationship between accumulative extraction and accumulative subsidence

subsidence curves (Helm 1976, 1984). As the factors influencing land subsidence are complex and geological conditions vary from place to place, a number of models have been established which have proved successful in particular situations (Qian 1981; Dassargues et al. 1993; Gu et al. 1995). Despite their increasing complexity, however, in practice many models fail to provide accurate predictions (Tianjin Center of Geological Survey 1991; Zhang 1991). There are two main reasons for this: the hydrogeological conceptual models used in the calculations cannot completely reflect the real geological conditions; and it is difficult to establish the correct parameters to be included. Shen et al. (1989) suggest that priority should be given to the resolution of these problems rather than the continual development of more complex models.

Using the characteristics of the land subsidence in Tanggu and the factual data obtained, a parameter optimization analysis method based on one-dimensional consolidation theory can be used to calculate stratum deformation. For this purpose, the measured stress-strain data were adopted and the deformation parameters of different subsidence stages determined as a function of time. The optimization analysis was used to infer the deformation of the soil layers, which were used with the deformation trends of the subsided strata in order to predict future subsidence.

Basic assumptions

1. The groundwater to induce land subsidence is 2D flow.
2. All additional stresses on the calculated confined aquifers originate from variations in the water table.
3. Pore water follows Darcy's law.
4. In weakly permeable beds the horizontal movement of ground water can be ignored.
5. In a single consolidation cycle the consolidation coefficients C_v and a_v of a compressed soil layer can be taken as a constant, although their value may be different in different consolidation cycles.

Calculation model

Calculation for sandy soil

As deformation of sandy soils can take place in a very short time and the situation can be restored equally quickly, elastic theory is appropriate. The suggested calculation model (Shen et al. 1989) is:

$$S \approx S_{\infty} = \frac{P_w \cdot g \cdot \Delta h}{E_s} \cdot M \tag{5}$$

where

S is stratum deformation (mm)
P_w is water density (Mg/m^3)
g is gravitation acceleration (9.81 m/s^2)
Δh is change in water head (m)
E_s is deformation module (MPa)
M is initial thickness of the sandy soil (m).

Calculation for clay soil and optimization of parameters

When dewatered, the deformation of clayey soil is mainly plastic. Such deformation can be considered as a one-dimensional problem for which Terzaghi's consolidation theory provides a simple calculation method. Its principal equation (Helm 1976) is:

$$\frac{\partial u}{\partial t} = C_v \frac{\partial^2 u}{\partial z^2} \tag{6}$$

where u is static pressure, t is time, C_v is the consolidation coefficient and z is depth.

If the effective stress increment (Δp) caused by the drop in the groundwater table (Δh) is used as an additional stress, the basic solution of the above equation is:

$$S_t = \frac{a_v}{1+e_0} \cdot p_w \cdot \Delta h \cdot M \cdot \left(1 - \frac{8}{\pi^2} \sum_{i=1}^{\infty} \frac{1}{(2i+1)^2} \cdot e^{-i^2 N}\right) \tag{7}$$

where $N = \frac{\pi^2 \cdot C_v}{4M^2} \cdot t$, S_t is deformation at time t, a_v is compression coefficient, e_0 is initial void ratio, M is soil thickness (in double-face pumping, take half of the soil thickness) and other symbols are the same as above.
Land subsidence is usually a long-term process, very different from laboratory conditions. In the different stages of the developing subsidence, the parameters change to some extent, hence it is difficult to determine parameters for calculating land subsidence from laboratory geotechnical test results. Where possible, deformation parameters should be calculated from measured field data. In the calculation of sandy soil deformation mentioned above, E_s can be obtained in this way, but in practice it was difficult to use this method to calculate deformation parameters for clayey soil. Equation (7) requires that the coefficients a_v and C_v must be known, but they cannot be obtained from measured data. If the deformation is short term and the data required small, repeated iteration could be an effective method to obtain these two parameters. However, if the deformation is over a long period and the data required are numerous, such iteration would not only be time-consuming but also unlikely to provide satisfactory results. In this case, optimization may be considered:

$$\min f(a_v, C_v) = \min\left\{\sum_{i=1}^{n}\left[S_m(a_v, C_v, \ldots, \Delta h_i, t_i) - S_v(\Delta h_i, t_i)\right]^2\right\} \quad (8)$$

where $f(a_v, C_v) = \sum_{i=1}^{n}\left[S_m(a_v, C_v, \ldots, \Delta h_i, t_i) - S_v(\Delta h_i, t_i)\right]^2$ is an object function which reflects the accumulative errors between calculated values and measured values, $S_m(a_v,C_v,\ldots,\Delta h_i,t_i)$ is a value obtained by "trial and error" for a set of iteration parameters, and $S_v(\Delta h_i,t_i)$ is the measured deformation corresponding to the difference in water table used in the iteration at time t_i.
The object of this optimization is to select a set of values for a_v and C_v which will minimize the value of the object function. The corresponding S_m is the optimization resolution of the stratum deformation. This is a "non-constraint optimization" problem which could be solved with the Direct Hooke-Jeeves Model Searching Method. This includes two searches: first to find the most favourable direction and then to accelerate the search along that line. The calculation process (Lin 1988) is as follows.
Given the initial value $x^{(0)}=(a_v{}^{(0)}\_C_v{}^{(0)}\ldots)$ and the step length $\delta>0$, and let k=0:
Stage 1:

starting from the base point $x^{(k)}$, search for a dropping point along a coordinate axis direction by the step length δ. If $e^{(i)}$ represents the ith coordinate axis direction, let

$$x^{(k+1,i)} = \begin{cases} x^{(k+1,i-1)} + \delta e^{(i)}\left(f(x^{(k+1,i-1)} + \delta e^{(i)}) < f(x^{(k+1,i-1)})\right) \\ x^{(k+1,i-1)} - \delta e^{(i)}\left(f(x^{(k+1,i-1)} - \delta e^{(i)}) < f(x^{(k+1,i-1)})\right) \le f(x^{(k+1,i-1)} + \delta e^{(i)}) \\ x^{(k+1,i-1)}\left(f(x^{(k+1,i-1)}) \le \min\left\{f(x^{(k+1,i-1)}) + \delta e^{(i)}), f(x^{(k+1,i-1)}) + \delta e^{(i)}\right\}\right) \end{cases} \quad (9)$$

where $x^{(k+1,0)}=x^{(k)}$, i=1, 2,...N. $x^{(k+1)}=x^{(k+1,n)}$ is named a new base point.
Stage 2:

let $x=x^{(k+1)}+[x^{(k+1)}-x^{(k)}]$. Starting from x, follow stage 1 and obtain $y^{(k+1)}$. If $f[y^{(k+1)}]<f[x^{(k+1)}]$, then let $x^{(k+1)}=y^{(k+1)}$ to complete an iteration, and again starting from stage 1, undertake the next iteration. If $f[y^{(k+1)}]\ge f[x^{(k+1)}]$, then reduce the step length (for example, $\delta\delta/2$ for $\delta\delta$) and begin again at stage 1 to a further iteration. The iteration process is complete when the step length is sufficiently small.

The combination of Eqs. (7) and (8) mentioned above provides a new way or model for calculating stratum deformation, referred to as the Optimization Model for Land Subsidence (OMLS; see Hu and Li 1994).

Results and discussion

Tianjin Alkali Mill was used to test the validity of this model. The present paper only demonstrates how to obtain the deformations of the clayey soil at the bottom and the sandy soil in the middle of the first confined aquifer, but the OMLS method can also be used with other similar soils. The depth of the bottom of the first confined aquifer is 83 m. Its total thickness is 59 m, of which 26 m is sandy soil and 33 m clayey soil. The stratigraphic structure of the first confined aquifer is shown in Table 2. The clayey soil occurs in two layers, either side of a sandy soil, with the lower clayey soil being 21 m thick. The total thickness of calculating strata (the confined sandy soil and the underlying clayey soil) is 47 m, at a depth of between 36 and 83 m below ground level. In both the sandy and clayey soils there were wire-flex extensometers, referred to as D_1 and D_2 respectively. A well to monitor the level of the groundwater level was also installed in each of the lithologies, T_{do1} and T_{do2}.
In the model, the annual change in the water table is taken as Δh of the sandy soil and the monthly change in the water table as Δh of the clayey soil. Table 3 gives the calculated results for the deformation parameters, while Fig. 14 shows the change in C_v and a_v from 1983–1997. Figure 15 shows the calculated and observed deformation related to the clayey soils. This indicates that the OMLS is an effective method for assessing the deformation and hence could be used to predict land subsidence. The elastic modulus and deformations for the sandy soils are computed separately in Figs. 16 and 17. In Fig. 17 it will be noted that the measured deformations have much higher peaks than the computed deformations. In the model, the

Table 2
Information on the first confined aquifer

Stratigraphic structure	Lithology	Depth of bottom of stratum (m)	Locations of wire-flex extensometers	Locations of water table monitoring boreholes	Ranges of calculated strata
Phreatic–slightly confined aquifer	Soft clay	24			
Confining bed	Clayey soil	36			
First confined aquifer	Sandy soil	62	ÿ_T_{do1}	ÿ_D_1	↕
Confining bed	Clayey soil	83	ÿ_T_{do2}	ÿ_D_2	

elastic modulus E_s is adopted in the rebound stage and E_c in the compression stage. In comparison with measured data, the calculated results generally have errors of less than 2 mm/year and are rarely as high as 5–6 mm/year. This suggests that using elastic theory for the sandy soils and considering the deformation difference between the compression stage and the rebound stage, the computed values may give a realistic indication of the overall deformation trend.
Table 3 is a summary of Figs. 14 and 17, reflecting generalized deformation indices for the clayey and sandy soils in the first confined aquifer. The deformations and relevant optimum parameters of other strata in the profile could be obtained using the method described above (Hu and Li 1994). Indeed, the land subsidence of the research area could be estimated by summing the deformations of all the strata in the profile:

$$S = \sum_{i=1}^{N} S_i \qquad (10)$$

Table 3
Optimizing deformation parameters (averaged)

Parameters	Compression stage	Rebound stage
a_v (cm^2/kg)	0.01377	0.00887
C_v (cm^2/s)	0.04837	0.02774
E (kg/cm^2)	2,482	13,107

where S is the total subsidence amount, S_i is the amount of deformation amount in a calculated layer and N is the number of strata.

Conclusions

In Tanggu, the groundwater within a depth of some 300 m has been extensively exploited, particularly the second and third confined aquifers which provide 46 and 24% of the total water extracted respectively. The land subsidence in this area has clearly been affected by the groundwater extraction, initially with a slow subsidence which accelerated with increased pumping and then reduced when mitigation measures were undertaken.
From the monitoring undertaken, the maximum subsidence is related to extraction from between 136 and 300 m, which accounts for some 65% of the total settlement. The effect of changes in the groundwater table varies for the two main soil types. For clayey soils the deformation takes place some time after the seasonal drop in groundwater level, but little restoration takes place when the water table rises. With the sandy soils, the deformation is mainly elastic without obvious hysteresis and the deformation correlates well with seasonal changes in the water table.
There is a significant correlation between accumulative groundwater extraction and accumulative subsidence. However, the same relationship is not found for annual

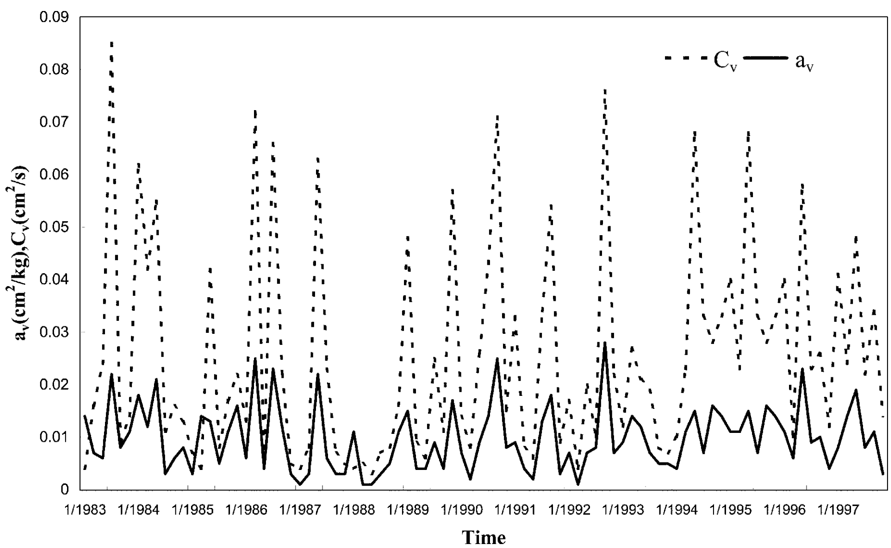

Fig. 14
Time-dependent curves of optimized deformation parameters of clayey soil: [a_v compression coefficient (cm^2/kg); C_v consolidation coefficient (cm^2/s)]

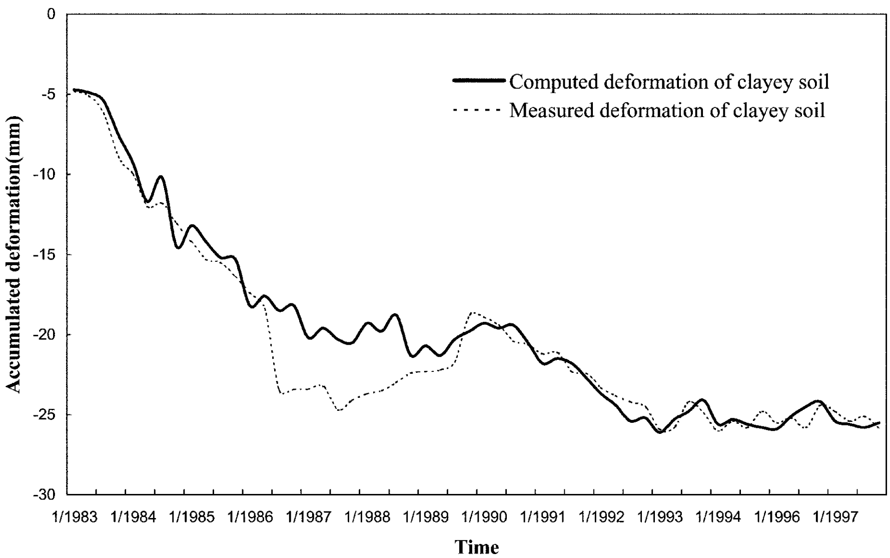

Fig. 15
Time-dependent curves of optimized deformations of clayey soil

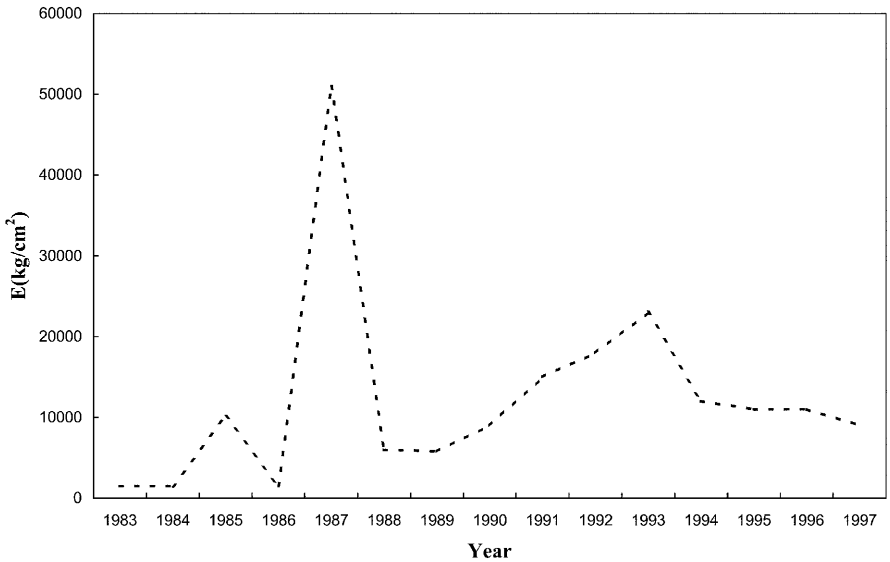

Fig. 16
Time-dependent curves of computed deformations of sandy soil

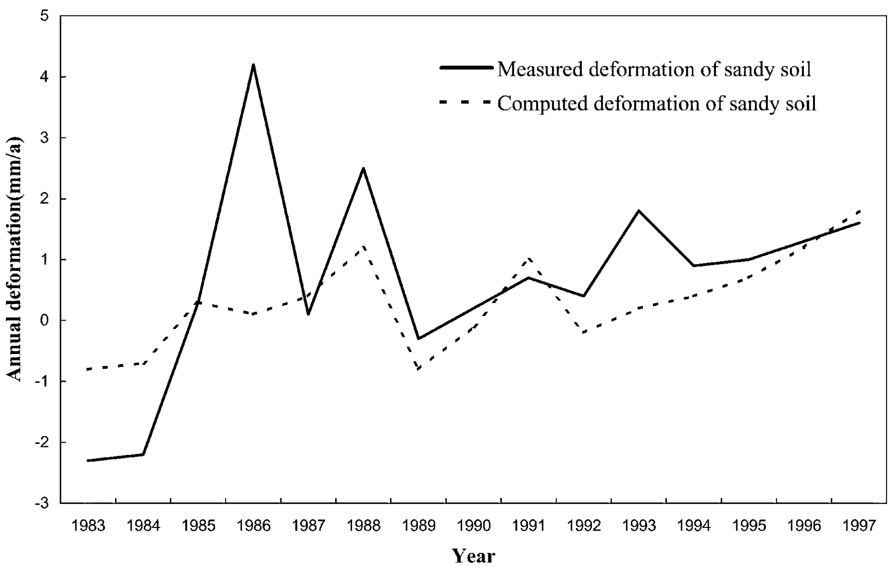

Fig. 17.
Time-dependent curve of inferred deformation modulus of sandy soil

extraction and annual subsidence, due to the hysteresis effect in the deformation of the clayey soil. A case study is presented to illustrate the application of an Optimization Model for Land Subsidence (OMLS). This indicates that the proposed model could be an effective method for calculating stratum deformation.

References

Dassargues A, Radu JP, Vharlier R, Li XL, Li QF (1993) Computed subsidence in the central area of Shanghai. Bull IAEG 47:27–50

Gu XY, Xu DE, Deng W (1995) A computing model based on cyclic consolidation tests. In: Barends FBJ et al. (eds) Proc 5th Int Symp on Land Subsidence, The Hague, Oct, IAHS Publ 234, pp 295–303

Helm DC (1976) One-dimensional simulation of aquifer system compaction near Pixley, California. 2. Stress dependent parameters. Water Resour Res 12(3):375–391

Helm DC (1984) Field-based computational techniques for predicting subsidence due to fluid withdrawal. In: Holzer TL (ed) Man-induced land subsidence. Reviews in Engineering Geology 6. Geological Society of America, Washington, DC, pp 1–22

Hu RL, Li XQ (1994) Modeling and prediction system for Beijing, Tianjin and Tangshan and its application prospect. China J Geol Disasters Their Prevention Control 5 (Suppl):120–127

Lin XY (1988) Modeling of quality and quantity of groundwater and a series of management programs. Jinlin Science and Technology Press, Jinlin, pp 10–60

Qian SY (1981) Calculation of land subsidence in Shanghai. J Rock Soil Eng 3(3):1–4

Shen XY, Sun SY, Li WF (1989) Physico-mathematical model and prediction of land subsidence in Ningbo City. Earth Sci 14(2):21–27

Tianjin Center of Geological Survey (1991) Report of exploration and prediction of land subsidence in Tianjin City (1980–1988). Tianjin Center of Geological Survey, Tianjin, pp 1–200

Xu DM, Yong RN, Mohamed AMO (1991) Time delay effect of subsidence. In: Johnson AI (ed) Land subsidence. IAHS Publ 200. Institute of Hydrology, Wallingford, pp 635–644

Zhang QZ (1991) Approach of factors of land subsidence and prevention in Tianjin urban area. In: Singh B, Saxena NC (eds) Proc In Symp on Land Subsidence, 11–15 Dec 1989, AA Balkema, Rotterdam, pp 639–658